Clinical and Translational Radiation Oncology 47 (2024) 100796

Contents lists available at ScienceDirect

Clinical and Translational Radiation Oncology

journal homepage: www.sciencedirect.com/journal/clinical-and-translational-radiation-oncology

Clinical evaluation of a deep learning CBCT auto-segmentation software for prostate adaptive radiation therapy

Lorenzo Radici [a], Cristina Piva [b], Valeria Casanova Borca [a], Domenico Cante [b], Silvia Ferrario [b], Marina Paolini [b], Laura Cabras [a], Edoardo Petrucci [a], Pierfrancesco Franco [c,d,*], Maria Rosa La Porta [b], Massimo Pasquino [a]

[a] Medical Physics Department, ASL TO4 Ivrea, Italy
[b] Radiotherapy Department, ASL TO4 Ivrea, Italy
[c] Department of Translational Sciences (DIMET), University of Eastern Piedmont, Novara, Italy
[d] Department of Radiation Oncology, 'Maggiore della Carità' University Hospital, Novara, Italy

ARTICLE INFO

Keywords:
Deep Learning
Auto-segmentation
Cone-Beam Computed Tomography
Prostate Cancer
Adaptive Radiotherapy

ABSTRACT

Purpose: Aim of the present study is to characterize a deep learning-based auto-segmentation software (DL) for prostate cone beam computed tomography (CBCT) images and to evaluate its applicability in clinical adaptive radiation therapy routine.

Materials and methods: Ten patients, who received exclusive radiation therapy with definitive intent on the prostate gland and seminal vesicles, were selected. Femoral heads, bladder, rectum, prostate, and seminal vesicles were retrospectively contoured by four different expert radiation oncologists on patients CBCT, acquired during treatment. Consensus contours (CC) were generated starting from these data and compared with those created by DL with different algorithms, trained on CBCT (DL-CBCT) or computed tomography (DL-CT). Dice similarity coefficient (DSC), centre of mass (COM) shift and volume relative variation (VRV) were chosen as comparison metrics. Since no tolerance limit can be defined, results were also compared with the inter-operator variability (IOV), using the same metrics.

Results: The best agreement between DL and CC was observed for femoral heads (DSC of 0.96 for both DL-CBCT and DL-CT). Performance worsened for low-contrast soft tissue organs: the worst results were found for seminal vesicles (DSC of 0.70 and 0.59 for DL-CBCT and DL-CT, respectively). The analysis shows that it is appropriate to use algorithms trained on the specific imaging modality. Furthermore, the statistical analysis showed that, for almost all considered structures, there is no significant difference between DL-CBCT and human operator in terms of IOV.

Conclusions: The accuracy of DL-CBCT is in accordance with CC; its use in clinical practice is justified by the comparison with the inter-operator variability.

Introduction

In modern external beam radiation therapy (RT) the main challenges, when treating prostate cancer, are the geometrical uncertainties due to set up and positional changes of both the prostate and surrounding organs at risk (OAR) [1].

During conventional RT, when the same treatment plan is being applied over the course of several weeks, treatment quality and dosimetric accuracy are potentially compromised due to intra and inter fraction changes. The intra-fraction residual motion of the prostate and seminal vesicles (SV) represents a relevant issue during treatment delivery [2]. Nevertheless, dosimetric deviations mainly arise from inter-fraction changes of either OAR volumes or relative distances between clinical target volume (CTV) and bladder or rectum [3].

To achieve the best outcome in terms of efficiency and accuracy, adaptive radiotherapy techniques (ART) have been introduced to ensure an accurate treatment delivery [4]. ART procedures include the actions taken to modify patient therapies, in case of discrepancies. Variations occurring during an ongoing fraction require an online ART strategy; an offline ART strategy is instead appropriate to define new irradiation

* Corresponding author: Department of Translational Medicine (DIMET), University of Eastern Piedmont, Via Solaroli 17, 28100 Novara, Italy.
E-mail address: pierfrancesco.franco@uniupo.it (P. Franco).

https://doi.org/10.1016/j.ctro.2024.100796
Received 29 October 2023; Received in revised form 9 May 2024; Accepted 16 May 2024
Available online 18 May 2024

criteria. When treating prostate patients, both ART strategies can be used to correct daily variations. Many steps in ART are dependent on fast and accurate OAR and target delineation on cone-beam computed tomography (CBCT). Auto-segmentation can reduce the workload for radiation oncologists and improve work efficiency.

Manual contouring on CBCT is a time-consuming process that limits the applicability of ART solutions. Therefore, deformable image registration (DIR) based methods, in which the structures contoured on the planning computed tomography (CT) are propagated on the CBCT via a DIR map, are widely used [5]. The performance of these methods is good within the limits of small deformations, while it may fail in presence of large deformations between the scans [6,7], such as in the pelvic region where changes in bladder and rectum filling frequently occur.

Recently, deep learning-based auto-segmentation become a mainstream support contouring techniques in CT [8,9]. Extending the use of deep learning algorithms to the contouring of structures on CBCT may contribute to mitigating the issues encountered with DIR based methods. Therefore, it may be appropriate to evaluate the applicability of these algorithms in the pelvic region.

However, the low image quality of CBCT, characterized by higher noise, artefacts and lower contrast for soft tissue compared to CT, can be a limiting factor for the application of deep learning algorithms [10,11]. In addition to limitations due to image quality, applications of deep learning techniques for CBCT segmentation are also limited by the scarcity of labelled images, necessary for training the algorithms. In fact, CBCT images are usually not contoured in clinical routine [12]. However, recent studies have shown promising results using hybrid deep learning-DIR [13,14] or only deep learning methods [12,15]. Furthermore, this approach is already integrated into the proprietary software of some Linac manufacturer, oriented toward the use of adaptive radiotherapy [16].

Several studies have described the clinical implementation of deep learning auto-segmentation software for CT [8,17,18]. Regarding deep learning CBCT auto-contouring, the currently published studies analyse different training methods for the neural networks [12,15,19–21]. However, evaluations of the clinical implementation of a deep learning CBCT auto-segmentation software have not yet been published.

Recently, a new deep learning auto-segmentation software implemented a beta version of auto-contouring of structures typically used in prostate treatments with an algorithm specifically trained on CBCT images. The application of this system for online or offline ART will depend on the degree of integration of the future clinical version, with pre-existing ART systems. However, the suitability in terms of performance will be necessary for its clinical use.

This is the first attempt to characterize the performance, in terms of accuracy and reliability, of this software for the automated contouring of prostate, seminal vesicles, femoral heads, bladder and rectum on CBCT images. Its performance on CBCT was compared against a gold standard consensus contour (CC). Furthermore, the accuracy was related to human inter operator variability (IOV) to evaluate its clinical applicability.

Material and methods

Deep learning-based auto segmentation

We used a commercial deep learning-based auto-segmentation software (DL) which uses deep convolutional neural network models based on a U-net architecture specific for each structure. DL technical details and training methods of the neural network have been already described [18]. DL for CT (DL-CT) images is validated by published studies that investigate its qualitative and quantitative accuracy and time savings [17,22,23]. A beta version (1.5.0-D2) is currently being developed to implement a contour model specifically trained on CBCT images (DL-CBCT). The CBCT model was trained using a combination of CBCTs from different linear accelerator manufacturers, coming from a variety of collaborating customers and publicly available datasets and implemented using TensorFlow [24]. Data augmentation and regularization techniques are used during training to improve model performance and prevent overfitting. Post processing of the contours, before the creation of a finalized structure set, includes outlier removal and contour smoothing. Further details of model generation and optimization methods used by DL have not been made public by the manufacturer.

DL obtains information related to the acquisition protocol by reading the DICOM metadata of the CT/CBCT images. The corresponding auto-segmentation model is automatically used to create auto-segmented contours that are exported alongside the CT/CBCT images to the Treatment Planning System (TPS) software.

Image acquisition and contouring

Ten patients, who received exclusive RT with definitive intent on the prostate gland and seminal vesicles, were selected in this study. A moderate hypofractionated schedule was employed: 70 Gy on the prostate gland and 63 Gy on the seminal vesicles in 28 fractions [25] delivered with a simultaneous integrated boost. All the patients were treated on a TrueBeam linear accelerator (Varian Medical Systems – A Siemens Healthineers Company, Palo Alto, CA, USA). CBCT scans were acquired by the on-board imager Varian Digital X-Ray imaging system with 125 kV_p half fan 360 degrees acquisition. The voxel resolution of the CBCTs were 0.9 mm × 0.2 mm × 2 mm.

One CBCT was selected for each patient (at fraction number 3) and four observers (expert radiation oncologists contourer – EC) independently delineated the prostate gland, seminal vesicles, femoral heads, bladder, and rectum. Operators were blinded to other operators' contours. All contours were segmented using Eclipse (Version 15.6) TPS contouring workspace.

Starting from these contours, a consensus contour was generated for each organ, using the simultaneous truth and performance level estimation (STAPLE) method [26] in the Computational Environment for Radiotherapy Research (CERR) software package [27]. These consensus contours were used as references for contour comparison analysis. The same CBCTs were contoured by DL using algorithms trained on both CBCT (DL-CBCT) and on CT (DL-CT).

Comparison of DL contours versus consensus contour

Multiple metrics, including Dice similarity coefficient (DSC), centre of mass (COM) shift and volume relative variation (VRV) were calculated to evaluate the segmentation accuracy of DL by comparing CC with both DL-CBCT and DL-CT. DSC [28] was used to quantify the overlap between the contours of DL-CBCT and DL-CT and CC. Let X and Y be two volumes to be compared, the coefficient DSC is defined as $DSC(X|Y) = 2|X \cap Y|/(|X|+|Y|)$. DSC values range from 0 for no overlap to 1 for complete overlap.

The centre of mass (COM) shift was evaluated in the three directions (X latero-lateral, Y cranio-caudal and Z antero-posterior direction). The absolute shift vector in 3D space was also evaluated to measure the displacement (mm) between CC and both DL-CBCT and DL-CT. All the metrics were obtained from the statistics tool of the contouring module of Varian Eclipse TPS. Furthermore, the DL contours were evaluated by the expert radiation oncologists and a qualitative description of the main differences was provided.

DL contours and inter-observer variability

Comparing the contours of DL-CBCT and DL-CT with respect to CC allows to quantitatively characterize its performances. However, as no tolerance limit can be defined for the used metrics, this analysis does not give a clear indication on the applicability of DL-CBCT to clinical routine. To study this possibility, the DL-CBCT performance was compared with the inter-operator variability (IOV) of 4 Radiotherapy

Oncologists, using the same metrics previously described. With this approach, the range of metric values for human-generated structures was used as reference for contour acceptability.

For each CBCT image set, DSC, absolute COM shift and VRV were evaluated between DL-CBCT and the four ECs resulting in multiple metrics values (DL-CBCT-EC) for each structure. Similarly, DSC, absolute COM displacement and VRV were measured between each EC pair, generating multiple EC-EC values to obtain an estimation of the IOV.

For DSC and COM, the average DL-CBCT-EC and EC-EC values for each case were used in the statistical analysis. Otherwise, in the case of VRV, the RMS was considered to account for the volume variations, regardless of their sign.

Statistical analysis was performed using the Wilcoxon signed-rank test to compare the DL-CBCT-EC distributions versus the EC-EC ones for each organ; p-values < 0.05 were considered statistically significant.

Results

Comparison of DL contours versus consensus contour

Femoral heads are the structures showing the best agreement between CC and both DL-CT and DL-CBCT. On average, DL-CBCT provides about 5 % ± 2 % (RMS 5 %) smaller volumes than CC while DL-CT contours are approximately 2 % ± 3 % (RMS 3.5 %) smaller than CC.

The mean femoral heads COM shift is less than 2 mm, for both DL-CT and DL-CBCT. The mean DSC for femoral heads contours is 0.96 ± 0.01 for both DL-CT and DL-CBCT.

Concerning the bladder, the mean VRV with respect to consensus contour is −2% ± 14 % (RMS 13 %) in the case of DL-CBCT and −9% ± 14 % (RMS 16 %) for DL-CT. The mean COM displacement is 2.2 ± 1.6 mm for DL-CBCT and 3.0 ± 2.0 mm for DL-CT. The mean DSC for bladder contours for all patients is 0.90 ± 0.06 and 0.89 ± 0.06 for DL-CBCT and DL-CT, respectively (Fig. 1).

In all cases the rectal volume contoured by DL is smaller than the STAPLE one. The rectal mean VRV is −15 % ± 10 % (RMS 18 %) and −13 % ± 20 % (RMS 23 %) for DL-CBCT and DL-CT, respectively. The mean COM shift for all patients is 3.8 ± 3.7 mm for DL-CBCT and 5.7 ± 5.9 mm for DL-CT. The mean DSC score is 0.86 ± 0.05 (DL-CBCT) and 0.81 ± 0.08 (DL-CT) (Fig. 1).

Regarding the qualitative assessment of the deep learning-generated contours by the expert radiation oncologists, the largest differences were found in the rectum segmentation for both DL-CT and DL-CBCT. Indeed, DL contoured rectum correctly included the anal canal caudally. However, cranially, the DL contour did not include the higher rectum, already outlined by DL as sigma. With respect to other organs at risk, expert radiation oncologists could not find any important difference. For example, DL contoured femoral heads correctly, stopping at the ischiopubical branch.

Table 1 summarizes the mean variation of the contour metrics for target volumes (prostate gland and seminal vesicles).

In the case of the prostate gland, the volume differences with respect to consensus contour for DL-CBCT and DL-CT are −11.8 % ± 14 % (RMS 17 %) and −11.5 % ± 23 % (RMS 25 %), respectively. Fig. 2 shows, for each patient, the mean COM shift (Fig. 2A) and the COM displacement in each direction for DL-CBCT (Fig. 2B). The mean prostate DSC for DL-CBCT is 0.83 ± 0.06 while for DL-CT it drops to 0.74 ± 0.10.

The seminal vesicles are the structures in which the largest differences between CC and both DL-CBCT and DL-CT have been found. DL-CBCT shows a mean volume reduction of about 21 % ± 23 % (RMS 30 %) compared to CC, a mean COM shift of 3.9 ± 4.0 mm and a mean DSC of 0.70 ± 0.16. The performances of DL-CT on seminal vesicles are lower. The mean change in volume is −40 % ± 24 % (RMS 46 %), with 50 % of patients having changes greater than 50 %. The COM shift is 6.8 ± 10.5 mm while the DSC is 0.59 ± 0.28. In Fig. 3, the performance of the results for OARs and CTVs contour are shown. Regarding the target volumes, the qualitative assessment could not show any specific pattern for DL.

DL contour and inter-observer variability

In Fig. 4, the EC-EC and DL-CBCT-EC distribution of DSC, COM shift and VRV RMS for femoral heads, rectum, bladder, prostate, and seminal vesicles is illustrated.

The statistical analysis shows that, for almost all the structures considered, there are no statistically significant differences between DL-

Table 1
Contour volume data variation, COM displacement and DSC for prostate and seminal vesicles.

	prostate		seminal vesicles	
	DL-CBCT	**DL-CT**	DL-**CBCT**	**DL-CT**
Volume [cc]	−7.8 ± 9.1	−7.9 ± 12.3	−6.1 ± 5.5	−9.7 ± 6.3
COM shift (Lateral) [mm]	−0.3 ± 0.8	−1.2 ± 1.3	0.5 ± 1.7	1.1 ± 2.4
COM shift (AP) [mm]	0.3 ± 1.5	3.3 ± 3.7	1.2 ± 4.6	5 ± 11
COM shift (Sup-Inf) [mm]	1.6 ± 1.9	1.7 ± 4.9	1.7 ± 2.0	0.9 ± 2.1
COM shift (Vector) [mm]	2.5 ± 1.6	6.1 ± 3.8	3.9 ± 4.0	6.8 ± 10.5
DSC	0.83 ± 0.06	0.74 ± 0.10	0.70 ± 0.16	0.59 ± 0.28

The value shown is the average value among all observers and patients. The value after ± represents one standard deviation.

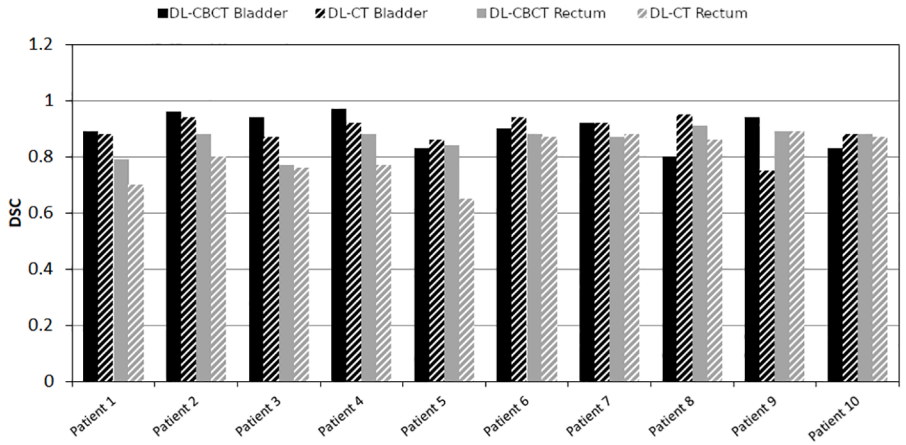

Fig. 1. DL-CBCT (black and grey) and DL-CT (dashed black and grey) DSC for bladder and rectum contours.

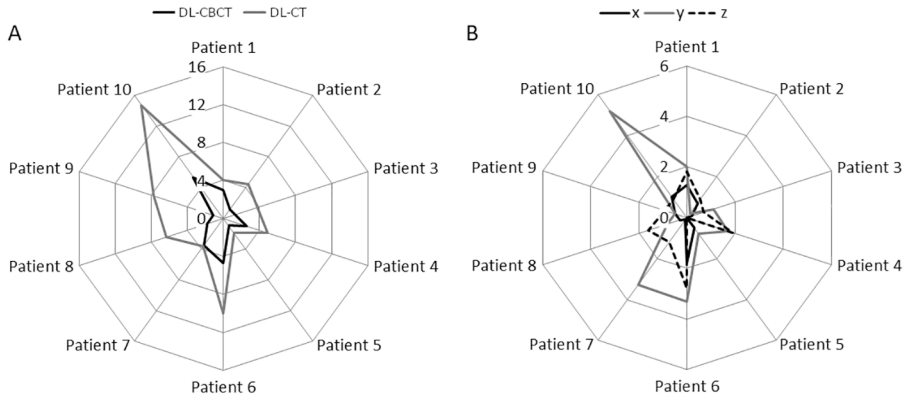

Fig. 2. Prostate COM shift [cm] with respect to CC for DL-CBCT (black) and DL-CT (grey) (A); COM displacement [cm] in x, y and z direction (B).

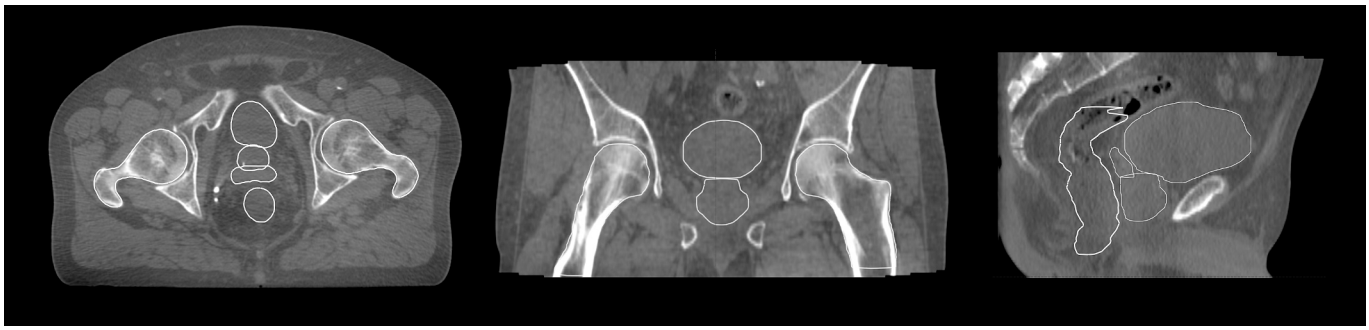

Fig. 3. Example of DL-CBCT contour.

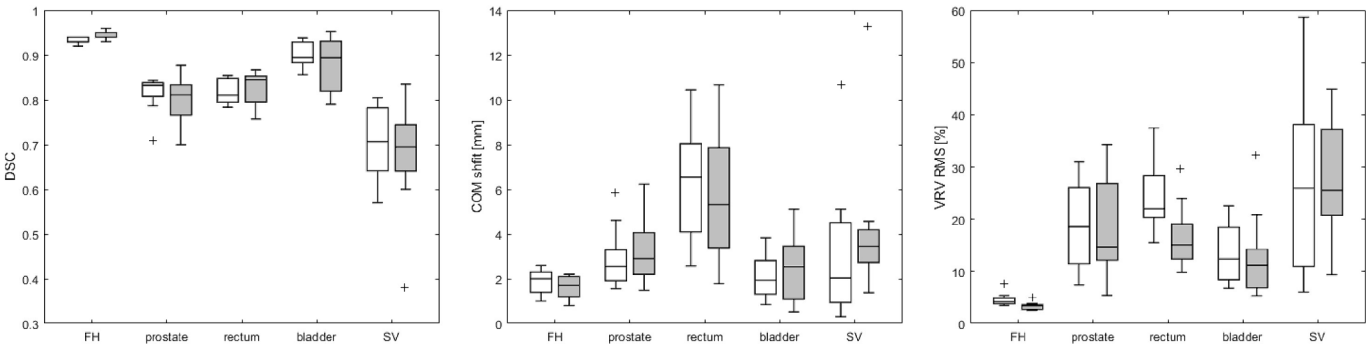

Fig. 4. EC-EC (white) and DL-CBCT-EC (grey) DSC, COM shift and VRV RMS boxplot distributions for Femoral Heads (FH), prostate, rectum, bladder and Seminal Vesicles (SV).

CBCT and human operator in terms of inter-operator variability. For DSC analysis, the only exception are the femoral heads, where there is a statistically significant difference (p-value < 0.01). However, the difference of median DSC between DL-CBCT-EC and EC-EC distribution is clinically not significant, with values of 0.94 and 0.93, respectively.

Similar results were found for COM shift. The distributions of the femoral heads show a statistically significant difference ($p = 0.02$), also for this metric. The median COM shift is 2.0 mm for EC-EC distribution and 1.7 mm for the DL-CBCT-EC one.

Concerning the analysis of VRV RMS, statistically significant differences were found for femoral heads and rectum ($p < 0.01$). As in the previous metrics, the DL-CBCT-EC distribution indicates a lower median variability than the EC-EC distribution. In particular, the median VRV RMS value for the rectum is 22 % for EC-EC and 15 % for DL-CBCT-EC. For femoral heads the median values are 4 % and 3 % for EC-EC and DL-CBT-EC, respectively.

Discussion

Recent studies have shown promising results for deep learning CT auto-segmentation of OARs and CTVs [8,29], with greater accuracy and time savings compared to atlas-based methods [30,31].

However, there are very few studies on CBCT-based soft tissue segmentation, primarily aimed at evaluating optimal training techniques [12,15,19,20].

The present study compares the performance of a beta version of a new commercial deep-learning based software, for auto-segmentation of the prostate gland, seminal vesicles, femoral heads, bladder, and rectum on CBCT images against a consensus contour, used as reference. Furthermore, the accuracy of DL-CBCT contours is validated against expert radiation oncologists inter observer variability.

With respect to OARs, the results show that the automatically generated contours are in general smaller than the manual reference contours. Lower discrepancies are obtained for DL-CBCT compared to

DL-CT, except for femoral heads. Moreover, for COM shift and DSC analysis, the best results are always obtained for DL-CBCT compared to DL-CT. These results suggest using algorithms specifically trained on the imaging modality of interest.

DSCs for femoral head, bladder and rectum are good. The analysis of DSC for CBCT images showed that the bladder achieved the best results (0.90 ± 0.06) compared to the rectum volume (0.86 ± 0.05). This relies on the general good contrast of the bladder in comparison to its surrounding tissue, except for the intersection with the prostate. DSC values for these OARs were similar to those found by Abbani et al. [20]: 0.91 ± 0.04 and 0.83 ± 0.06 for bladder and rectum respectively. Leger et al. [15] tested different training approaches for a deep learning segmentation algorithm; their best results, compared to a single human operator, showed a DSC of 0.874 ± 0.096 and 0.814 ± 0.055 for bladder and rectum, respectively. A similar approach has also been described by Fu et al. [21]. In their study, a DSC of 0.96 ± 0.03 and 0.93 ± 0.08 was reported for bladder and rectum, respectively. Schreier et al. [19] found a DSC of 0.932 and 0.871 for bladder and rectum. However, their analysed image set contains both CT and CBCT. All the previous publications did not compare the auto segmented contours with a consensus contour. Therefore, the results do not explicitly consider the variability related to the single human operator.

A consensus contour approach was instead used by Gardner et al. [32]. In their study, the performance of a DIR based CBCT segmentation approach was evaluated. The inter-operator variability compared to a STAPLE CC on CBCT was also analysed. In the case of the bladder, a DSC of about 0.95 and 0.85 was found for human and DIR propagated contours, respectively. Concerning the rectum, a DSC of about 0.85 and 0.75 was found for human and DIR propagated contours, respectively. The previously described inter-operator variability results are compatible with the performance of DL-CBCT, also with respect to the literature data.

Regarding the COM shift of the organs at risk, the rectum exhibited the largest value (3.8 mm), which could be mainly identified in the cranial region. A similar behaviour, with variations of up to 2 mm in the z-direction for the rectum, was found by Lütgendorf-Caucig et al. [33] by analysing the inter-operator variability on CBCT.

Regarding target volumes, the performance of the system specifically trained on CBCT is superior to that of the algorithm trained on CT and used for CBCT segmentation.

The most significant variations between DL-CBCT and CC were observed for the prostate gland in the superior-inferior direction (1.6 ± 1.9 mm). A possible explanation may be that the physicians contoured the prostate slice-by slice in the axial view. Due to the low image contrast of the prostate in the CBCT image, it is a challenge for the clinician to distinguish whether the prostate is seen via a single axial view in the inferior direction, resulting in a large CC uncertainty. Similar results were found by Gardner et al. [32]. The prostate COM shift of human contoured CBCT versus a consensus contour was 2.01 ± 0.46 mm, with the main contribution seen in the superior-inferior direction.

The prostate DSC result for DL-CBCT (0.83) is consistent with other deep learning algorithms reported in the literature: Schreier et al. [19] found a DSC of 0.84, Abbani et al. [20] described a DSC of 0.85 ± 0.04. Furthermore, the prostate DSC value was shown to align with the inter-operator variability described by Gardner et al. [32] (DSC = 0.872 ± 0.05).

Due to the small size of the SVs, a small change in shape definition has a great influence on the DSC values. In fact, the SVs show the lowest DSC value (0.70 ± 0.16) among all structures, comparing DL-CBCT contour to that of the consensus. This result is similar to that of Schreier et al. [19] (0.70). Furthermore, Lütgendorf-Caucig et al. [33] found a high variability in the contouring of the seminal vesicles on CBCT, although they use slightly different parameters.

Because of the lower soft tissue contrast, this organ is the most difficult to contour for both human and auto-segmentation algorithms within the entire pelvic body site.

More generally, it is observed that the largest discrepancies between manual and deep learning-based organ structures occurred because of insufficient contrast at organ interfaces.

Comparing the performance of DL-CBCT over CBCT versus the data of DL-CT over CT reported in the literature [17 23], it is noted that they are comparable with respect to DSC and volume variation for bladder, rectum and femoral heads, while a slight worsening (of about 2 mm) of DL-CBCT on CBCT is found with respect to the COM shift of bladder and rectum.

Inter-observer variability for contouring is a widely analysed source of uncertainty [34] for planning CTs. Fewer studies are present for CBCT segmentation [33], however there is an indication of a higher IOV in the case of CBCT.

The use of DL-CBCT in clinical practice can be justified by the comparison with the inter-operator variability. As highlighted in Fig. 4, for most of the structures and metrics used, DL-CBCT does not change the department inter-operator variability. Moreover, in cases of statistically significant differences between EC-EC and DL-CBCT-EC distributions, the comparison shows a reduction in variability for DL-CBCT-EC. This fact shows that DL-CBCT contours have not significant variations compared to human contours, indicating a substantially robustness.

Furthermore, since the department IOV is at least qualitatively comparable with that of other publications [32,33], the previous evaluations can be generalized to other situations.

An accurate review by a human expert operator is however always necessary. In fact, the delineations of organs such as the prostate and seminal vesicles can follow different indications than the simple anatomical conformation when contoured as CTV, depending on the clinical needs. Furthermore, although DL-CBCT has shown comparable performances to a human operator, some errors have been noted.

In conclusion, the accuracy of DL trained on CBCT images is in accordance with CC and comparable to expert IOV for the RT structures analysed in this study. The clinicians are required to review or perform minor/major correction on the structures.

Furthermore, it is necessary to point out that we tested a beta version of a software whose clinical release will be forthcoming. It is possible that some features will be further optimized in the official version.

However, for application in online ART, adequate integration between the clinical version of the auto-segmentation software and the online imaging and dose calculation system will be required. Additionally, in the case of dose calculation on CBCT images, there are problems related to the assignment of electron density, the size of the field of view of the CBCT images and, more generally, the reconstruction of synthetic CT images [35].

Moreover, our sample, limited to 10 CBCTs, only allows for a preliminary evaluation that could show the appropriateness of this beta release and suggests an adjunctive analysis when the clinical version will be available.

Even so, the use of DL CBCT segmentation in clinical practice most likely will lead to significant benefits to the RT planning workflow and resources. Hence, these results are encouraging for the adoption of automated deep learning-based segmentation software into the clinical workflow as a step towards the clinical implementation of ART, to simplify and optimize the segmentation process of organs at risk necessary for a quantitative dosimetric evaluation.

Funding: none

Data statement

Research data are stored in an institutional repository and will be shared upon request to the corresponding author.

Declaration of competing interest

The authors declare that they have no known competing financial interests or personal relationships that could have appeared to influence the work reported in this paper.

References

[1] Barney BM, Lee RJ, Handrahan D, Welsh KT, Cook JT, Sause WT. Image-guided radiotherapy (IGRT) for prostate cancer comparing kV imaging of fiducial markers with cone beam computed tomography (CBCT). Int J Radiat Oncol Biol Phys 2011; 80(1):301–5. https://doi.org/10.1016/j.ijrobp.2010.06.007.

[2] Litzenberg DW, Balter JM, Hadley SW, et al. Influence of intrafraction motion on margins for prostate radiotherapy. Int J Radiat Oncol Biol Phys 2006;65(2): 548–53. https://doi.org/10.1016/j.ijrobp.2005.12.033.

[3] Peng C, Ahunbay E, Chen G, Anderson S, Lawton C, Li XA. Characterizing interfraction variations and their dosimetric effects in prostate cancer radiotherapy. Int J Radiat Oncol Biol Phys 2011;79(3):909–14. https://doi.org/10.1016/j.ijrobp.2010.05.008.

[4] Posiewnik M, Piotrowski T. A review of cone-beam CT applications for adaptive radiotherapy of prostate cancer. Phys Med 2019;59:13–21. https://doi.org/10.1016/j.ejmp.2019.02.014.

[5] Oh S, Kim S. Deformable image registration in radiation therapy. Radiat Oncol J 2017;35(2):101–11. https://doi.org/10.3857/roj.2017.00325.

[6] Thor M, Petersen JB, Bentzen L, Høyer M, Muren LP. Deformable image registration for contour propagation from CT to cone-beam CT scans in radiotherapy of prostate cancer. Acta Oncol 2011;50(6):918–25. https://doi.org/10.3109/0284186X.2011.577806.

[7] Zambrano V, Furtado H, Fabri D, et al. Performance validation of deformable image registration in the pelvic region. J Radiat Res 2013;54(Suppl 1):i120–8. https://doi.org/10.1093/jrr/rrt045.

[8] Samarasinghe G, Jameson M, Vinod S, et al. Deep learning for segmentation in radiation therapy planning: a review. J Med Imaging Radiat Oncol 2021;65(5): 578–95. https://doi.org/10.1111/1754-9485.13286.

[9] Isaksson LJ, Summers P, Mastroleo F, et al. Automatic segmentation with deep learning in radiotherapy. Cancers (basel) 2023;15(17):4389. https://doi.org/10.3390/cancers15174389.

[10] Lechuga L, Weidlich GA. Cone beam CT vs. fan beam CT: A comparison of image quality and dose delivered between two differing CT imaging modalities. Cureus 2016;8(9):e778. https://doi.org/10.7759/cureus.778.

[11] Scarfe WC, Farman AG. What is cone-beam CT and how does it work?. 707-v Dent Clin North Am 2008;52(4). https://doi.org/10.1016/j.cden.2008.05.005.

[12] Brion E, Léger J, Barragán-Montero AM, Meert N, Lee JA, Macq B. Domain adversarial networks and intensity-based data augmentation for male pelvic organ segmentation in cone beam CT. Comput Biol Med 2021;131:104269. https://doi.org/10.1016/j.compbiomed.2021.104269.

[13] Liang X, Morgan H, Bai T, Dohopolski M, Nguyen D, Jiang S. Deep learning based direct segmentation assisted by deformable image registration for cone-beam CT based auto-segmentation for adaptive radiotherapy. Phys Med Biol4 2023;68. https://doi.org/10.1088/1361-6560/acb4d7. Published 2023 Feb 10.

[14] Ma L, Chi W, Morgan HE, et al. Registration-guided deep learning image segmentation for cone beam CT-based online adaptive radiotherapy. Med Phys 2022;49(8):5304–16. https://doi.org/10.1002/mp.15677.

[15] Léger J, Brion E, Desbordes P, De Vleeschouwer C, Lee JA, Macq B. Cross-domain data augmentation for deep-learning-based male pelvic organ segmentation in cone beam CT. Applied Sciences 2020;10(3):1154. https://doi.org/10.3390/app10031154.

[16] Moazzezi M, Rose B, Kisling K, Moore KL, Ray X. Prospects for daily online adaptive radiotherapy via ethos for prostate cancer patients without nodal involvement using unedited CBCT auto-segmentation. J Appl Clin Med Phys 2021; 22(10):82–93. https://doi.org/10.1002/acm2.13399.

[17] Radici L, Ferrario S, Borca VC, et al. Implementation of a commercial deep learning-based auto segmentation software in radiotherapy: evaluation of effectiveness and impact on workflow. Life (Basel) 2022;12(12):2088. https://doi.org/10.3390/life12122088.

[18] Wong J, Fong A, McVicar N, et al. Comparing deep learning-based auto-segmentation of organs at risk and clinical target volumes to expert inter-observer variability in radiotherapy planning. Radiother Oncol 2020;144:152–8. https://doi.org/10.1016/j.radonc.2019.10.019.

[19] Schreier J, Genghi A, Laaksonen H, Morgas T, Haas B. Clinical evaluation of a full-image deep segmentation algorithm for the male pelvis on cone-beam CT and CT. Radiother Oncol 2020;145:1–6. https://doi.org/10.1016/j.radonc.2019.11.021.

[20] Abbani N, Baudier T, Rit S, et al. Deep learning-based segmentation in prostate radiation therapy using Monte Carlo simulated cone-beam computed tomography. Med Phys 2022;49(11):6930–44. https://doi.org/10.1002/mp.15946.

[21] Fu Y, Lei Y, Wang T, et al. Pelvic multi-organ segmentation on cone-beam CT for prostate adaptive radiotherapy. Med Phys 2020;47(8):3415–22. https://doi.org/10.1002/mp.14196.

[22] Wong J, Huang V, Giambattista JA, et al. Training and Validation of Deep Learning-Based Auto-Segmentation Models for Lung Stereotactic Ablative Radiotherapy Using Retrospective Radiotherapy Planning Contours. Front Oncol 2021;11:626499. https://doi.org/10.3389/fonc.2021.626499.

[23] Zabel WJ, Conway JL, Gladwish A, et al. Clinical evaluation of deep learning and atlas-based auto-contouring of bladder and rectum for prostate radiation therapy. Pract Radiat Oncol 2021;11(1):e80–9. https://doi.org/10.1016/j.prro.2020.05.013.

[24] Pang B, Nijkamp E, Wu YN. Deep learning with tensorflow: A review. J Educ Behav Stat 2020;45(2):227–48.

[25] Girelli G, Franco P, Sciacero P, et al. Image-guided intensity-modulated radiotherapy for prostate cancer employing hypofractionation and simultaneous integrated boost: results of a consecutive case series with focus on erectile function. Anticancer Res 2015;35(7):4177–82.

[26] Warfield SK, Zou KH, Wells WM. Simultaneous truth and performance level estimation (STAPLE): an algorithm for the validation of image segmentation. IEEE Trans Med Imaging 2004;23(7):903–21. https://doi.org/10.1109/TMI.2004.828354.

[27] Deasy JO, Blanco AI, Clark VH. CERR: a computational environment for radiotherapy research. Med Phys 2003;30(5):979–85. https://doi.org/10.1118/1.1568978.

[28] Dice LR. Measures of the amount of ecologic association between species. Ecology 1945;26(3):297–302.

[29] Guo H, Wang J, Xia X, et al. The dosimetric impact of deep learning-based auto-segmentation of organs at risk on nasopharyngeal and rectal cancer. Radiat Oncol 2021;16(1):113. https://doi.org/10.1186/s13014-021-01837-y.

[30] Ibragimov B, Xing L. Segmentation of organs-at-risks in head and neck CT images using convolutional neural networks. Med Phys 2017;44(2):547–57. https://doi.org/10.1002/mp.12045.

[31] Lustberg T, van Soest J, Gooding M, et al. Clinical evaluation of atlas and deep learning based automatic contouring for lung cancer. Radiother Oncol 2018;126 (2):312–7. https://doi.org/10.1016/j.radonc.2017.11.012.

[32] Gardner SJ, Wen N, Kim J, et al. Contouring variability of human- and deformable-generated contours in radiotherapy for prostate cancer. Phys Med Biol 2015;60 (11):4429–47. https://doi.org/10.1088/0031-9155/60/11/4429.

[33] Lütgendorf-Caucig C, Fotina I, Stock M, Pötter R, Goldner G, Georg D. Feasibility of CBCT-based target and normal structure delineation in prostate cancer radiotherapy: multi-observer and image multi-modality study. Radiother Oncol 2011;98(2):154–61. https://doi.org/10.1016/j.radonc.2010.11.016.

[34] Fiorino C, Reni M, Bolognesi A, Cattaneo GM, Calandrino R. Intra- and inter-observer variability in contouring prostate and seminal vesicles: implications for conformal treatment planning. Radiother Oncol 1998;47(3):285–92. https://doi.org/10.1016/s0167-8140(98)00021-8.

[35] Giacometti V, Hounsell AR, McGarry CK. A review of dose calculation approaches with cone beam CT in photon and proton therapy. Phys Med 2020;76:243–76. https://doi.org/10.1016/j.ejmp.2020.06.017.